Egyptian Veterinary Medical Society of Parasitology Journal

Behour et al. EVMSPJ 2015; 11:1-11

Original Article

Molecular Analysis and Histopathological Alterations During the Evolution of *Trypanosoma evansi* Infection in Experimentally Infected Mice

Tahani S Behour[1], Shawki M Aboelhadid[2], Waheed MA Mousa[3], Selim A Selim[4], Adel S Amin[1]

[1]Biotechnology Research Unit, Animal Reproduction Research Institute, Giza, Egypt

[2]Parasitology Department, Faculty of Veterinary Medicine, Beni Suef University, Egypt

[3]Parasitology Department, Faculty of Veterinary Medicine, Cairo University, Egypt

[4]Pathology Department, Animal Reproduction Research Institute, Giza, Egypt

Abstract:

The aim of the current study is to follow up *Trypanosoma evansi* infection in experimentally infected mice by the parasitological and molecular assays. Also, the pathological alterations in different tissues associated with the infection throughout the course of disease were investigated. Forty two male and forty two female Swiss mice were injected I/P by 10^2 trypanosomes and five mice for each group were kept as non infected control. The course of infection was followed up by direct microscopic examination and PCR assay for *T. evansi* RoTat 1.2 VSG gene. Pathological changes were also estimated through the disease progression by examination of thin sections from formalin fixed tissues and staining with haematoxylin and eosin. Results revealed earlier detection of *T. evansi* in mice blood by PCR at 24 h post-infection while direct microscopic examination revealed that the pre-patent period was five days. During the chronic course of the disease, when the parasite disappeared from the blood by direct microscopic examination, PCR assay gave positive signals for the parasitic DNA in the blood. Histopathological examination revealed that *T. evansi* induced destructive irreversible damage of the mice vital organs (kidneys, liver, spleen, brain and testes) especially in chronic infection and lead to death of the animals with progression of the disease. It also affects animals' fertility. It induces degenerative changes in the testes and seminiferous tubules.

Key words: *T. evansi*, mice, PCR, tissues, Pathology, Infertility

INTRODUCTION

Surra, insect borne disease, is a serious disease caused by haemoprotozoan *T. evansi*. It has the widest host range among salivarian trypanosomes. The parasite spreads mechanically by haematophagous insects and infects both domestic and wild animals but the most pathogenic effects were recorded in camels, equids and dogs **(OIE, 2012; Rjeibi et al., 2015)**. The pathogenic effects of *T. evansi* include fever, anaemia, loss of appetite and condition, nervous signs, abortion, neonatal mortality, weakness and death **(Gardiner and Mahmoud, 1990)**.

The major problem of the disease is affecting animal productivity and fertility, with undetectable spread of infection. Notably, these signs are variable in severity, from totally unapparent to lethal between and within a host species, depending on the geographical area or the epidemiological situation **(Desquesnes et al., 2013; Al-Shabbani et al., 2013)**. The histopathological alterations are not characteristic for the disease **(Dargantes et al., 2005b)**. Degenerative changes developed in tissues of the host are resulted from deprivation of glucose which utilized by the parasite for its motility, survival and multiplication **(Bal et al., 2012)**. The parasite also is able to induce immunosuppression allowing small trypanosome population to evade the protective immune responses and remain clinically silent in the host resulting in anthroponotic reservoir **(Desquesnes et al., 2013)**. Lacking of rapid and reliable diagnostic method resulted in misdiagnosis of the disease. Although identification of *T. evansi* can be performed by conventional parasitological tests or by DNA based techniques however PCR methods are the most reliable and sensitive for diagnosis of *T. evansi* infection **(Sengupta et al., 2010; Bal et al., 2012)**.

As *T. evansi* is highly pathogenic for laboratory animals **(Bal et al., 2012)**, the aim of the study is to detect the pathological changes in different tissues associated with *T. evansi* infection throughout the course of the disease in experimentally infected Swiss mice in addition to detection of *T. evansi* by polymerase chain reaction assay using specific primer.

Materials and Methods

Experimental Design

Trypanosoma evansi strain used in this study was kindly provided by Parasitology Department, Faculty of Veterinary Medicine, Cairo University as experimentally infected mice. The parasite was expanded in Swiss mice by I/P inoculation of infected mice blood. Preservation of the parasite in liquid nitrogen was carried out according to **Shumei et al. (1996)** till used as a positive control in the molecular analysis.

Forty seven adult males and forty seven females Swiss mice of approximately 30 gm of weight were used in the study. The mice were divided into two groups according to their sex. The first group (group I): forty two male mice were kept separately and inoculated I/P by 102 *Trypanosoma evansi* (infective dose) according to **Sharma et al. (2012)** and the other 5 mice were kept isolated as non infected control group. The same design was done with the female group (group II). Three mice from each group were examined daily by preparing wet blood smear from peripheral blood according to **Brener (1962)** then sacrificed and the blood was collected on anti-coagulant for molecular examinations.

The process was started from the first day post infection to detect the pre-patent period till peaking parasitemia (over 100 *T. evansi*/ microscopic field x 40). After peaking parasitemia, all mice were examined twice weekly by wet blood smear for assessment of parasitemic waves along the course of infection. During the chronic waves which started after peaking parasitemia till the end of the experiment, mice blood and tissues (livers, spleens, kidneys, ovaries, testes and brains) were collected and divided into two parts, one parts of those organs preserved at -20°C for molecular analysis and the other part was fixed in 10% neutral buffered formalin for histopathological examinations.

DNA extraction from blood and tissue samples:

DNA was extracted from positive control (*T. evansi* strain), and from each blood sample according to **Sarataphan et al. (2007)** with some modifications in tissues. Briefly, 50 µl of each whole blood sample was lysed twice in 500 µl of 0.1 M ammonium chloride. After centrifugation, the sediment was resuspended in 50 µl of 0.002% sodium dodecyle sulphate and 50 µl of 5% chelex-100® (Sigma) suspension in TE buffer (10 mM Tris-HCl, 0.1 mM EDTA, pH 8.0). The mixture was heated at 70°C for 8 minutes followed by heating to 100°C for 10 minutes. Finally, after centrifugation at 10,000 rpm for 5 min at room temperature, the supernatant was stored at -80°C for PCR analysis. For tissues, 0.5 gm of each tissue was washed in 500 µL of phosphate buffer saline then the tissue was grinded in liquid nitrogen till became powder. Pellet suspended in 300 µL of 10% chelex-100® suspension in TE buffer. Then samples were processed as described previously in blood extraction.

DNA amplification by conventional PCR assays:

For detection of *T. evansi* DNA, PCR analysis was done by using primer pair TeRoTat920 F - TeRoTat1070 R **(Konnai et al., 2009)** in standard PCR procedures. The primer pair amplifies a DNA fragment of 151 bp. Optimization of PCR components and conditions was done using *T. evansi* camel isolate which propagated in mice and cryopreserved as positive control. The PCR mixture of 25 µl was optimized to contain 2X PCR Dream Taq TM Green PCR Master Mix (2x) (Fermentas, life science), 25 pmol of each primer, 2 µl of DNA template and up to 25 µl Nuclease free water were added. PCR using TeRoTat920 F- (5' CTG AAG AGG TTG GAA ATG GAG AAG 3') and TeRoTat1070 R (5' GTT TCG GTG GTT CTG TTG TTG TTA 3') were performed in a thermocycler (eppendorf thermal Cycler, Germany) for initial denaturation at 95°C for 4 minutes, 35 cycles of denaturation at 95°C for 60 s, annealing at 52°C for 60 s, and extension at 72°C for 60 s and final extension at 72°C for 10 minutes. Amplicons were resolved on a 1.5% agarose gel stained with ethidium bromide (Sigma) and photographed under UV light **(Sambrook and Russell, 2001)**. Positive control (*T. evansi* DNA) and negative control (reaction mixtures without DNA) were included in each PCR run.

Histopathological examinations:

The fixed tissue samples in 10% neutral buffered formalin were processed and embedded in paraffin according to the standard procedures described by **Luna (1986)**. Thin sections of 4 µm thickness were prepared and stained with hematoxylin and eosin (H&E) according to **Carleton et al. (1967)** for demonstration of the pathological changes using light microscope.

Results

Follow up the parasitemia in experimentally infected mice by wet blood smear:

In both groups, *T. evansi* appeared in the blood of mice experimentally infected with 102 trypomastigote after

prepatent period of 5 days. The peak of parasitemia was recorded at 9 days post infection. At the peak of parasitemia (over 100 *T. evansi*/ microscopic field x40), in group I (male group) 18 mice were died while 3 mice showed disappearance of the parasite from blood (chronic stage) at the fifteenth day PI (Fig. 1 males' group G1). The other 6 mice were died during the period from 9th to the 22nd days PI from persistent parasitemia (chart 1 males' group G2). In group II (female group) by teaming parasitemia, three-group patterns were observed, the first pattern was 6 mice showed persistent parasitemia and died within the 12th to 34th days post- infection (G1). The second pattern was other 6 mice showed disappearance of parasitemia at the 15th day PI and remained stable till the end of the experiment (G2) (at the 46th day). The third pattern (represented by the rest of mice) showed 3 waves of parasitemia at the 9th, 22nd and 34th days post-infection. These waves were alternated by 3 waves of aparasitemia at the 15th, 29th and 46th days PI (G3) (Fig. 1 females' group).

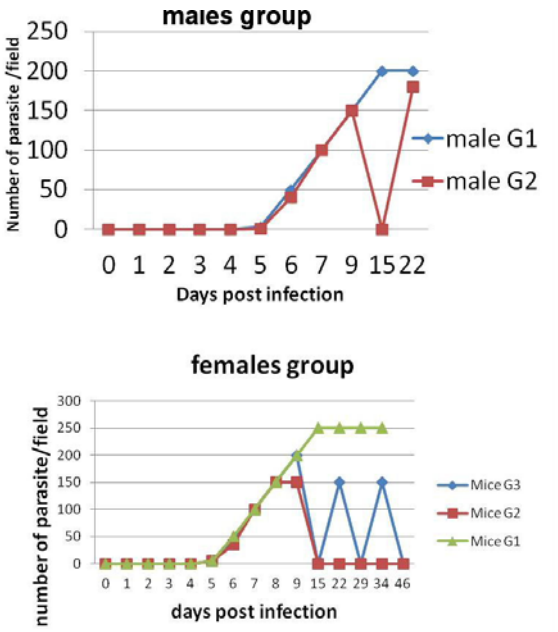

Figure 1: The course of the parasitemia and chronic waves in both males and females' mice groups by direct microscopic examination of wet blood smear. The plotted curves represent the different disease patterns obtained in experimentally infected mice during the experiment.

Molecular detection by Conventional PCR:

Detection of *T. evansi* in mice blood:

By application of PCR on mice blood results revealed early detection of *T. evansi* DNA at 24 hours post infection in both groups using RoTat1.2 with amplified fragment size 151bp (Fig. 2). The assay was able to detect *T. evansi* DNA from the first day post-infection in both groups (Fig. 2). The intensity of the amplified bands was clearly observed increased gradually from the beginning of the experiment and throughout the course of infection correlated with parasite load in the mice blood. Moreover, examination of blood collected during the chronic phase (15 and 29 DPI) by PCR revealed clear identification of 151 bp DNA amplified products using RoTat1.2 primers (Fig. 3).

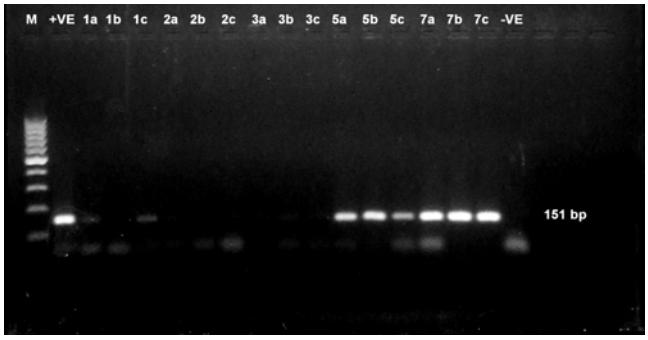

Figure 2: PCR on blood of mice injected by 10^2 trypanosome with RoTaTat 1.2 primer sets for detection of the pre-patent period. Lanes M: 100bp molecular weight DNA marker. +ve: positive control.-ve: negative control. Numbers: days post infection. Letters: mice scarified at that day.

Detection of *T. evansi* in mice tissues:

Genomic DNA extracted from different frozen mice tissues (liver, spleen, kidneys, testes/ovaries and brain) collected at 7, 15, 29 and 46 days post infection showed amplification 151 bp DNA fragment (Fig. 4). The assays revealed positive results in both parasitemic (7 DPI) and chronic waves (15, 29, and 46) in all collected tissues.

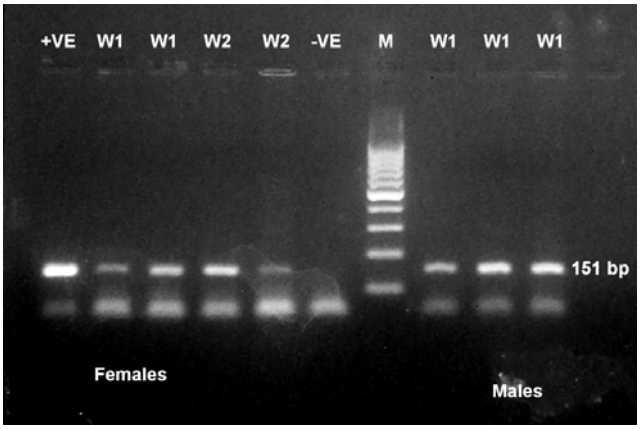

Figure 3: Detection of T. evansi in mice blood during the chronic phase by PCR. Lanes M: 100 bp molecular weight DNA marker, +ve: positive control, -ve: negative control, W1: first wave (fifteenth DPI) and W2: second wave (twenty ninth DPI) .

Histopathological changes:

Histopathological examination of the non-infected control group did not show any pathological changes in the all examined tissues. In experimentally infected groups, variable prominent pathological changes were seen

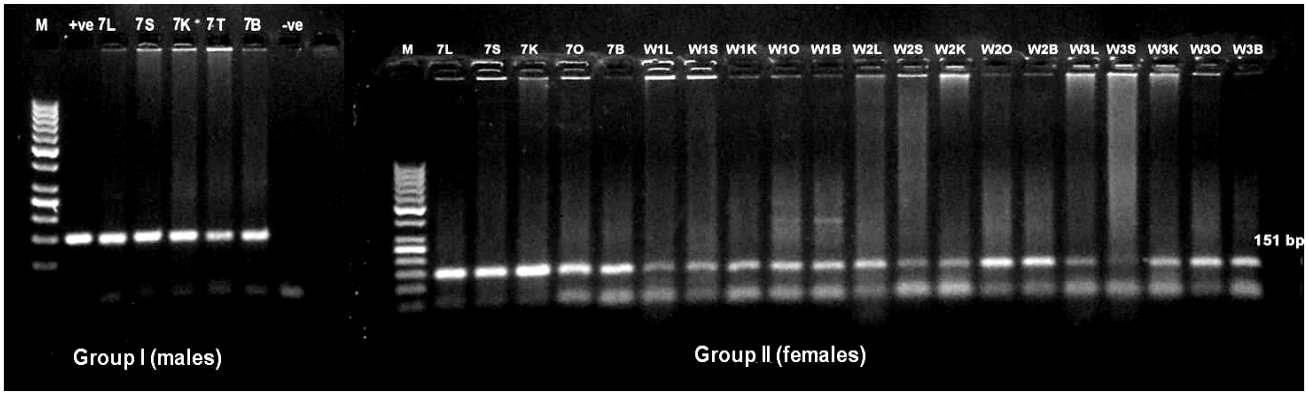

Figure 4: PCR amplification of DNA extracted from tissues of infected mice using TeRoTat primer set. M: 50 bp molecular weight DNA marker, +ve: positive control, -ve: negative control, 7: days post infection, W1: chronic wave (15 DPI), W2 (29 DPI), W3 (46 DPI) and L (liver) S (spleen) K (kidney) T (testicle) O (ovary) B (brain).

through the course of infection and according to the sex of mice.

Kidneys

At parasitemia (7 DPI), kidneys showed granular and vacuolar degeneration of the epithelium of some uriniferous tubules, mild congestion and focal infiltrations of mononuclear inflammatory cells with limited small hemorrhagic area. Also, necrobiotic changes of epithelial cells of few uriniferous tubules were recorded in addition to focal areas of edema infiltrated with mononuclear inflammatory cells (Fig. 5A). By the first wave of parasite disappearance (15 DPI), sporadic glomeruli get shrinked with pyknosis of glomerular tuft cells that increased in the second wave at 29 DPI (Fig. 5B). Renal tissues revealed prominent vacuolar and granular degenerative changes with shrinkage glomeruli accompanied with focal perivascular mononuclear cells infiltration in the third wave at 46 DPI in addition to renal casts.

Liver

During parasitemia (7 DPI) liver revealed diffuse vacuolar degeneration of hepatocytes with focal aggregations of inflammatory cells particularly around the portal areas. Prominent diffuse mononuclear inflammatory cells appeared within the sinusoids with activation of Kupffer's cells. At 15 DPI, Multiple diffused necrotic hepatocytes were observed particularly around dilated portal veins

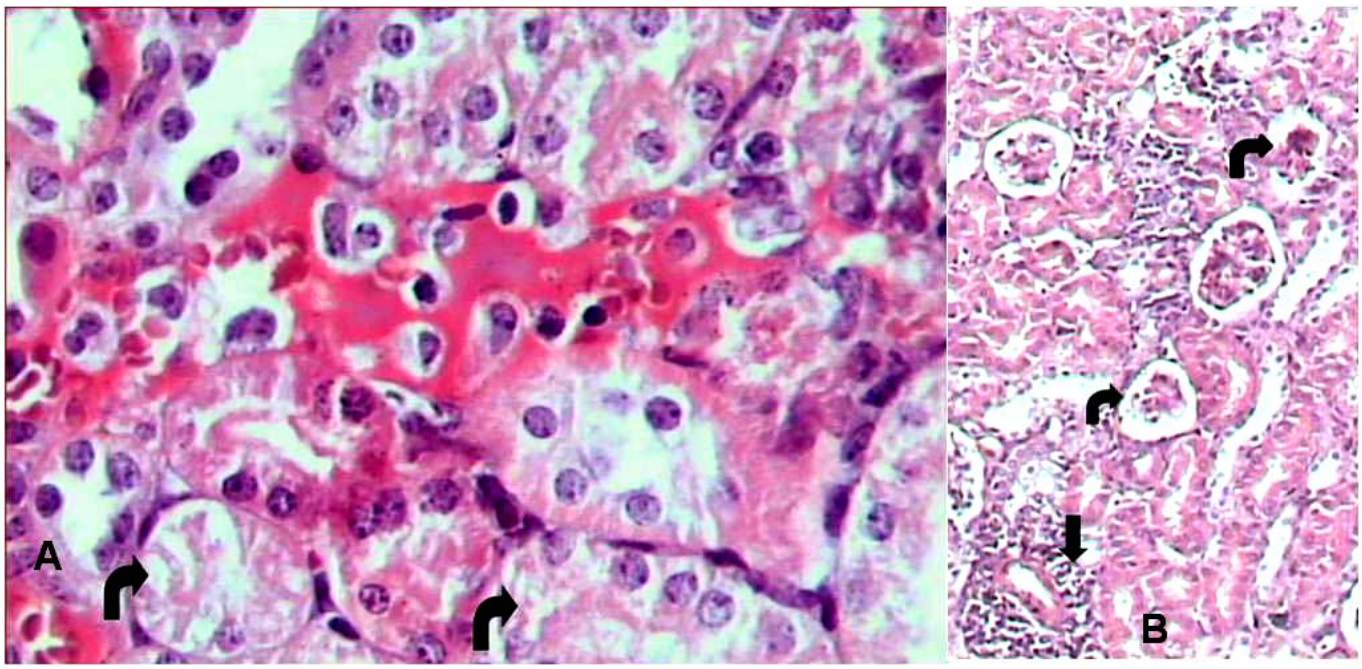

Figure 5: A: Kidney of female mice during parasitemia showed Granular and vacuolar degeneration of uriniferous tubular epithelium with Necrobiotic changes of some cells (bent arrow), Focal area of edema infiltrated with mononuclear inflammatory cells. x40.
B: Kidney of male mice at the first chronic wave (15 DPI) showed inflammatory cells infiltrations around blood vessels (down arrow), marked shrinked glomeruli (bent arrow) with degenerative changes in uriniferous tubular epithelium. x10.

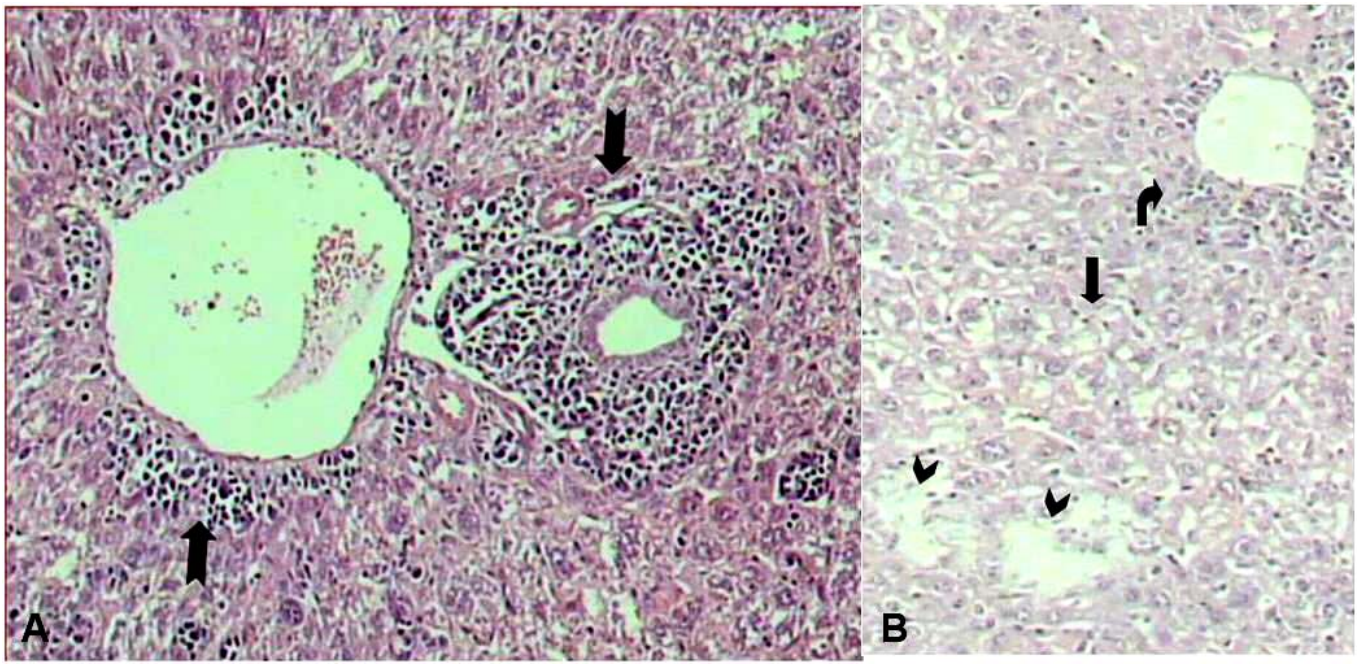

Figure 6: A: Liver of female mice during first chronic wave (7 day PI) showed: Diffuse vacuolar degeneration of hepatocytes with focal aggregation of inflammatory cells. Aggregation of inflammatory cells around the portal area (down notched arrow) and central veins (up notched arrow). x10. **B**:Liver of male mice at chronic wave (15 day PI) showed: Diffused vacuolar degeneration (down arrow), focal areas of complete lyses of hepatocytes leaving vacuoles in their sites (arrows heads) (liver vacuolation), central veins surrounded by focal aggregation of mononuclear inflammatory cells (bent arrow) and activation of von Kupffer cells. x10.

and that were replaced by mononuclear inflammatory cells (Fig. 6A). At the end experiment (46 DPI), some central veins surrounded by focal aggregation of mononuclear inflammatory cells were recorded. In males at 15 DPI, notably those focal areas of complete lyses of hepatocytes were recorded throughout the course leaving space in their sites (liver cavitations) (Fig. 6B).

Spleen

Spleen follicles appeared large with narrow germinal center. They were less prominent from splenic parenchyma due to follicular hypertrophy and high cellularity of splenic red bulb during parasitemia (7 DPI). Vacuolar degenerative changes appeared in the splenic parenchymal cells (Fig. 7A). Some cells appeared pyknotic with large histiocytes and few giant cells. Moreover,

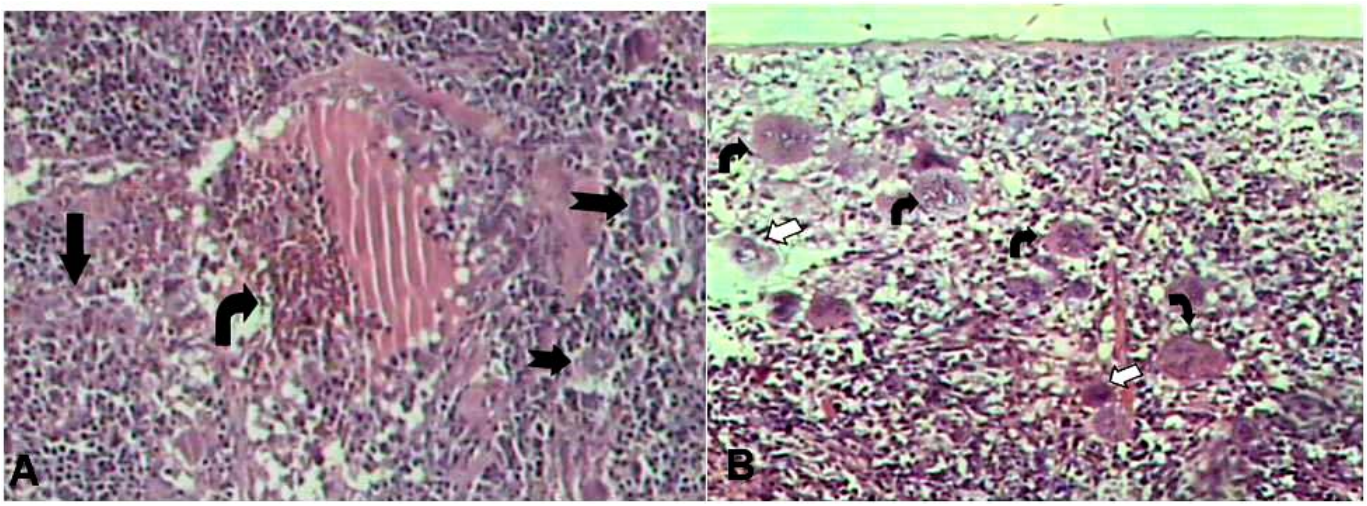

Figure 7: A: Spleen of male mice during parasitemia (7 day PI) showed: Less prominent follicles with narrow germinal center (down arrow), increased number of large macrophages (right notched arrows) with some multinuclear giant cells with multiple small necrotic areas and edema (bent arrow). Necrotic areas showed pyknotic, karyolitic nuclei with nuclear debris. x10. **B**: Spleen of female mice during the first chronic wave (15 day PI) showed: Prominent large macrophages (white arrows) and giant cells (black bent arrows) at subcapsular area with vacuolar degenerative changes in reticular stromal cells. x10

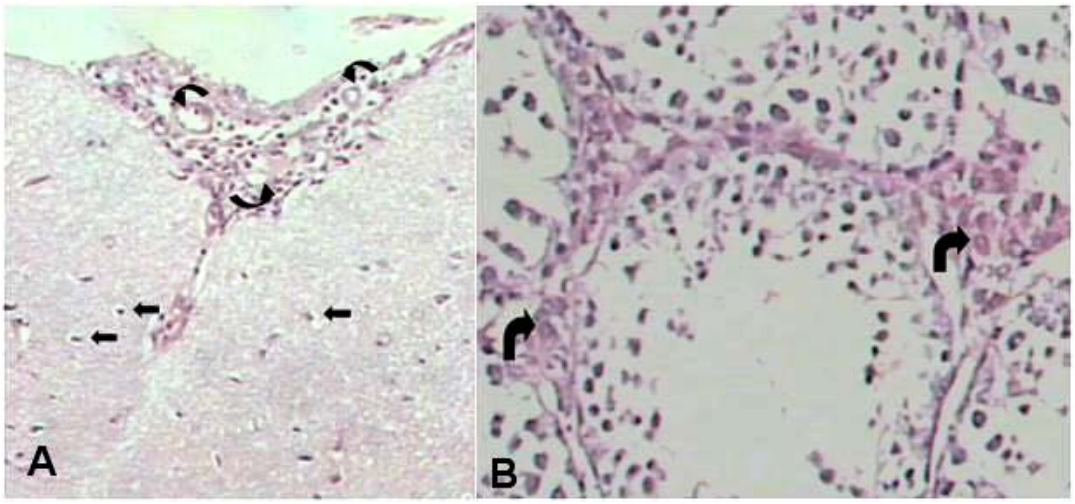

Figure 8: A: Brain tissue of male during the first chronic wave (15 day PI) showing meningitis with dilated meningeal blood vessels (curved arrows) and moderate infiltration of mononuclear inflammatory cells were observed. Pyknotic neural cells with pericellular edema (left arrows) were seen in the tissue of cerebral cortex. x10. **B:** Testes of male mice during parasitemia (7 day PI) showed: Leydig cells were prominent and showing open phase nucleus (bent arrows), degeneration of spermatogonial mother cells with few desquamated germinal epithelial cells. x10

multiple necrotic areas in the splenic parenchyma associated with exudative edema in male tissues. At 15 days post infection, prominent large histiocytes particularly at the sub-capsular area were appeared with vacuolar degenerative changes in the reticular cells and mild congestion in blood vessels (Fig. 7B). At the second wave (29 DPI), multiple giant cells and histiocytes were more prominent. At the end of the course (46 DPI), the follicles were well observed with multiple giant cells but without congestion.

Brain

Brain showed mild perivascular edema with collapsed blood vessels at 7 DPI. Sometimes focal necrotic areas were seen with appearance of pericellular edema. In addition, focal hemorrhage infiltrated with neutrophils and sporadic degenerated neurons with neuronophagia were also seen at 15 DPI. Focal mild meningitis with mononuclear inflammatory cells infiltrations and mild congestion were observed (Fig. 8A).

Testes and Ovaries

No significant pathological changes were observed in ovaries however in testes many pathological changes were recorded. At the seventh day post infection, spermatogenic cells appeared normal although 80% of seminiferous tubules were empty from sperms. Then, sporadic seminiferous tubules showed degeneration of spermatogonial mother cells and about 20% showed desquamation of germinal epithelium. Leydig cells were prominent and showed open phase nuclei (Fig. 8B). Mild congestion of blood vessels was recorded. In the chronic phase (15 DPI), about 60% only of seminiferous tubules showed sperms.

DISCUSSION

For well estimation of medical and economic impacts of *T. evansi*, identification of the etiological agent and evaluation of its pathogenic effects and impact are important. Unfortunately, the clinical and pathological signs of *T. evansi* infected animals are not pathognomonic resulting in difficulty and misdiagnosis of the disease. Therefore, searching for rapid, sensitive and accurate laboratory method is necessary to facilitate diagnosis **(Dargantes et al., 2005b; Desquesnes et al., 2013)**. For definitive diagnosis for surra, demonstration of trypanosomes in tissues or blood of the hosts is required; however it influenced by the parasitemia level and viability of trypanosomes in blood or tissue samples. Parasitological tests are helpful in detecting *T. evansi* in infected animals with high parasitemia but diagnostic issues appear in chronic disease in which animal exhibits very low parasitemia. Trypanosomes in samples from animals with high and low parasitemia (>104 and 250 trypanosomes mL-1 of blood) could not be detected beyond 8 and 3 hours after storage at 4°C and 27°C respectively to maintain viability of trypanosome in blood and should not be exposed to direct sunlight **(Nantulya, 1990; Holland et al., 2001a)**.

PCR-based assays are described as powerful tools for the detection of *T. evansi* in several animals and vectors

(Sukhumsirichart et al., 2000). Sample processing does not have to be done within minimum time after collection but can be delayed at least 180 days after preservation at -20° C **(Abdel-Rady, 2008)**. Moreover, the assays are not only able to detect and amplify parasite nucleic acids with high sensitivity and specificity but also able to distinguish different species involved **(Dávila et al., 2003)**.

Variant surface glycoprotein (VSG) covered the surface of Trypanosome is the main antigenic determinant to the host immune system. The parasite is able to periodically switch its coat to evade the host immune response and produce waves of parasitemia. There are 1000 genes encoded in the genome for VSG. These genes are randomly switched on and off at each generation resulted in antigenic variation of *T. evansi* **(Bacchi, 2009)**. *T. evansi* RoTat 1.2 VSG gene is a specific DNA region lacking homology to other known VSG genes in trypanosomes, but it is highly conserved among *T. evansi* strains **(Claes et al., 2004)**. It is expressed in early, middle and late stages during the disease evolution. So, it is recommended in early diagnosis, follow up and determination of carrier status in *T. evansi* infection **(Sengupta et al., 2010)**.

In this study, TeRoTat 1.2 primer set was chosen for applying the PCR assay to detect the pre-patent period and follow up the course of the infection in the experimentally infected mice along with direct microscopic examination of wet blood smear. Results showed that the pre-patent period was 120 hours (five days) post infection by 102 trypanosomes in both groups (males and females) by direct microscopic examination while by using PCR, the pre -patent period was estimated 24 hours post infection with amplification of 151 bp DNA fragment. **Sharma et al. (2012)** detected the parasite at 108 h and 72 h after inoculation of 102 parasites by examination of wet blood smear and real time PCR assay respectively after experimental infection of *T. evansi* in mice. Differences in the pre-patent periods arises from many factors includes species difference, host susceptibility, pathogenicity of the isolate, route and dose of infection and the test used to detect parasitemia **(Dargantes et al., 2009)**.

Survival durations in current study were recorded in males' mice 12- 22 days however in females' mice, survival times were stretching 12- 46 days. Different survival durations were recorded by many researchers; **Shama et al. (2012)** (10 -14 days) in mice inoculated with 102 trypomastigotes, **Carmona et al. (2006)** (12-24 days) in mice inoculated with 1 trypomastigote/g body weight. **Mekata et al. (2012)** inoculated mice with 103 trypo-mastigotes and obtain survival duration of 9- 20 days. **Shams El-Din (2012)** obtained 11.2 days as the mean survival time of mice inoculated with 4.5x 105 with overall mortality within 30 days. **Mekata et al. (2013)** recorded 19.8 days as a mean of survival days of 60% from mice inoculated with 2.0×103 purified parasites. The other 40% of mice were survived till 30 days and authors didn't show whether mice were sacrificed or died. **Tejero et al. (2008)** inoculated mice with 1 trypomastigote/g of body weight and mice revealed a distinctive adulatory-like parasitemic pattern that resembles waves for 39 days. Moreover, **Araque (1985)** found in his study that two mice strains were able to overcome the acute phase with survival times up to 60 days. The variation in survival time of mice inoculated with *T. evansi* may be attributed to the strain virulence, host susceptibility, inoculated dose and environmental factors. In this study environmental temperature was critical factor for mice survival. Animals infected with *T. evansi* are characterized by fluctuating parasitemia resulted from the interaction of the immune response of the host and the ability of the parasite to evade it by antigenic variation. These waves of parasitemia are accompanied by the rise and fall of the body temperature of the host **(Dargantes et al., 2009)**. During these periods, demonstration of *T. evansi* in animal blood is efficient while at times when parasitemia is low, detection of the parasite is difficult making diagnosis a problem.

In the current study, PCR was more reliable in accurate detection of the parasite in mice blood during aparasitemic waves (chronic stage) in both males and females however examination of wet blood smear could not due to very low number of the parasite present in the blood. **Ashour et al. (2013)** and **Ramirez-Iglesias et al. (2011)** obtained the same results in experimental mice and rabbit infection respectively. Our finding indicated the usefulness of PCR not only for early diagnosis of *T. evansi* infection, but also for detecting the chronically infected animals with very low parasitemia and act as a focus for the spread of infection. **Ramírez-Iglesias et al. (2012)** and **Desquesnes and Davila (2002)** referred the only limitation of using PCR during the first days post infection to absence of *T. evansi* in the examined sample since the sensitivity of the assay has been reported of or less than 1 parasite/ml blood by **Sengupta et al (2010)**.

The histopathological alterations associated with *T. evansi* infection is not characteristic unless in the presence of the parasite in the investigated tissues is confirmed **(Dargantes**

et al., 2005b). In the current study, detection and identification of *T. evansi* in the tissues collected during both parasitemic and chronic waves of the disease was performed by PCR. Results revealed amplification of the specific 151 bp DNA fragment using TeRoTat 1.2 specific primer set in all examined mice tissues (livers, spleens, kidneys, ovaries, testes and brains) throughout the course of infection. Positive results from amplification of 400 bp DNA fragments of *T. evansi* in mice tissues experimentally infected with the parasite using specific primer set targeting VSG gene were previously reported by **Sengupta et al (2010)**.

Destructive effect and the cellular pathological lesions associated with *T. evansi* infection are described as complications of the interaction between the host immune system and the parasite mechanisms to evade the immune response of the host **(Dargantes et al., 2005a)**. Immune complexes, cytokines (interferon, interleukins, chemokines and tissue necrotic factors) and nitric oxide are considered the products resulted from that interaction and played the major role in the cellular damage in infected host **(Baral et al., 2007; Saleh et al., 2009)**. Other studies related the degenerative changes in the host to reduction of oxygen and glucose required for the cells by its consumption for parasite growth and multiplication in addition to toxins produced by the parasite **(Bal et al., 2012)**. Generally, the pathological changes caused by trypanosomoses are influenced by many factors as host species, type of isolate, infective dose, stage of infection and some environmental factors **(Dargantes et al., 2005b)**.

In the current study, renal pathological changes were represented by degeneration and necrosis in glomerular tuft which became shrinkage with appearance of renal casts at renal tubules by the end of the course. Epithelium of uriniferous tubules showed necrobiotic changes. Also, mild congestion and focal infiltrations of mononuclear inflammatory cells with edema and limited small hemorrhagic areas were observed. Previous studies inferred the renal alterations to the presence of parasite or its toxins **(Surynarayana et al., 1986)** and the immunological response of the host **(Uche and Jones 1992)** which impairs the structure and function of kidneys. They illustrated the mechanism of destruction of tissues that inducted glomerulonephritis allowed deposition of antigen-antibody complexes which damage tubular epithelium followed by tubular necrosis and atrophy. Presence of hemorrhagic lesions increased the release of immuno-complexes and elevated the tubular epithelium damage **(Biswas et al., 2001)**. Thus, occurrence of sudden death may be due to acute renal failure and kidney damage which was observed in the male mice group when reaching parasitemia. **Biswas et al. (2001)** reported the same changes in Bandicoot rat and they were the first researchers mentioned the shrinkage of glomerulus which recorded in this study. In liver, the most vital organ, vacuolar degenerative changes and necrosis of hepatocytes indicated chronic trypanosomosis which were irreversible pathological changes and lead to death of the infected animals as occurred in this study specially in the male mice group **(Biswas et al., 2001)**.

Severe destructive changes were recorded in the male infected group as focal areas of complete lyses of hepatocytes were seen producing liver cavitations. The necrosis of hepatocytes particularly around portal area at early stages indicates the toxic effect of the trypanosome metabolites while, the late necrosis of hepatocytes particularly around central veins indicate the hypoxic and the hypoglycemic effect. This is coincided with **Bal et al. (2012)** who stated that, the degenerative changes in the host were resulted from reduction of oxygen and glucose required for the cells by its consumption for parasite growth and multiplication in addition to toxins produced by the parasite. **Biswas et al. (2001)** inferred the necrosis of hepatocytes around dilated portal veins and that were replaced by mononuclear inflammatory cells to the presence of toxins in the plasma and tissue fluid which stimulate secretion of lysosomes. Produced lysosomal vesicles in a cell coalesce and form a large vesicle and when this lysosomal vesicle bursts. Autolysis of the takes place and initiate the necrotic process.

Focal aggregation of mononuclear inflammatory cells around some central veins may be due to hypoglycemia and hypoxemia resulted from consumption of glucose and oxygen by trypanosomes for their motility and multiplication resulting in degenerative changes in hepatocytes **(Uche and Jones 1992; Bal et al., 2012)**. Activation of Kupffer cells with diffuse mononuclear inflammatory cells appeared within the sinusoids were suggested to be related to increased breakdown of red blood cells and intense antigenic stimulation **(Anosa and Kaneko 1984)**. Death of animals also may be due to immunosuppression resulted from failure of the immune system to recognize the secondary infection antigens. This

can be attributed to the impairment of complement component (C3) production which is the most important component for activation of the complement pathway **(Uche and Jones, 1992)**.

In spleen, follicular hypertrophy and high cellularity of splenic red bulb and vacuolar degenerative changes appeared in the splenic parenchymal cells. By progression of the disease, multiple necrotic areas in the splenic parenchyma associated with exudative edema in male tissues were appeared. Then multiple giant cells due to aggregation of histiocytes were more prominent. **Biswas et al. (2001)** and **Bal et al. (2012)** obtained the same pathological changes in the spleen in experimentally infected Bandicoot rats and mice respectively. **Uche and Jones (1993)** referred the splenic damage to immediate hypersensitivity to *T. evansi.* However, **Surynarayana et al. (1986)** related splenic pathological changes in donkeys to the anemic anoxia resulted from the presence of *T. evansi* and its toxic metabolites.

Brain showed focal necrotic areas with appearance of pericellular edema, mild perivascular edema with collapsed blood vessels. In addition, focal hemorrhage infiltrated with neutrophils and sporadic degenerated neurons with neuronophagia were also seen. With disease progression, focal mild meningitis with mononuclear inflammatory cells infiltrations and mild congestion were observed. **Bal et al. (2012)** reported that the pathological changes occurred in the brain were induced by presence of parasite or its toxic metabolites and supported the idea by demonstration of the parasite in blood vessels of the brain of infected animals. Otherwise, **Sackey (1998)** inferred the degenerative changes of the brain to the formed immune complexes instead of cell mediated immune reaction. It was found that no significant pathological changes were observed in ovaries of infected female mice however positive signals for presence of parasite were obtained from the ovarian tissues by PCR assay. In contrast, **Faccio et al. (2013)** observed an increase in the concentration of NO (Nitric Oxide), AOPP (Advanced Oxidation Protein Products), and TBARS (Thiobarbituric Acid Reactive Substances) in the ovaries of rat experimentally infected with *T. evansi*, which was indicative of cell damage.

In Testes, seminiferous tubules showed degeneration of spermatogonial mother cells. Most seminiferous tubules showed aspermia and desquamation of germinal epithelium. Leydig cells were prominent and showed open phase nuclei with mild congestion of blood vessels. **Hemeida et al (1985)** revealed varying degrees of spermatogenic arrest, collapsed Sertoli cells and normally functioning Leydig cells in degenerated dromedary testicles.

Anti-fertility effect of *T. evansi* in Black Bengal bucks was detected by **Pradhan et al. (2013)** after examination of testicular tissue section which showed diffuse degeneration of spermatogonia and Sertoli cells, lacking of spermatozoa and proliferation of fibrous connective tissue in intertubular spaces. Pathological alterations in testes including aspermia were reported by previous authors in male goats **(Dargantes et al., 2005b)**, horses **(Ikede et al., 1983)**, rabbits **(Chandra et al., 1999)** and camels **(Hemeida et al., 1985)**. Male infertility induced by *T. evansi* infection was supported by **Tizard (1996)** and **Al-Qarawi et al. (2004)**. They elucidated the mechanism as immune complexes resulted from variable surface glycoproteins of *T. evansi* precipitated under the basement membrane of the seminiferous tubules in the chronically infected males leading to interference of the biological functions of junctional complexes, impaired metabolism or hyperactivation of the Sertoli cells and elevated plasma estradiol-17β concentrations. Later, higher concentration of estrogen suppresses secretion of gonadotropin-releasing hormone (GnRH) and causes a negative feed-back mechanism on luteinizing hormone (LH) leading to depression in Leydig cell function and maintaining low levels of plasma testosterone. Both trypanosoma-induced immune complexes and hormonal defects could impair the sequential divisions and differentiation of germ cells to produce spermatozoa. In current study, Leydig cells were noticed functional however about 80% of seminiferous tubules were empty. This may be explained as; investigation was occurred early before the occurrence of the negative feed back mechanism. Also, *Trypanosoma evansi* infection was contributed to infertility in male rats either directly by causing marked testicular damage and morphological disorders in sperms or indirectly by reduction of serum levels of reproductive hormones **(Faccio et al., 2014)**.

In conclusion, *T. evansi* induces destructive irreversible damage of the mice vital organs especially in chronic infection and lead to death of the animals with progression of the disease. It also affects animals' fertility specially males which can cause considerable economic

losses. Thus, as verified in this study, finding an accurate, sensitive, reliable method such as PCR will not only detect the early infection of *T. evansi* introduced to the animals but also it able to discriminate the chronically infected carrier ones. So understanding of the course of the disease and finding suitable diagnostic tool will help good estimation of medical and economic impacts of the disease to encourage its prevention and control.

REFERENCES

Abdel-Rady, A. (2008): Epidemiological studies of Trypanosoma evansi infection in camels (Camelus dromedarius) in Egypt. Veterinary World, 11: 325-328.

Al-Qarawi, A.A. Omar, H.M. Abdel-Rahman, H.A. El-Mougy, S.A. and El-Belely M.S. (2004): Trypanosomiasis-induced infertility in dromedary (*Camelus dromedarius*) bulls: changes in plasma steroids concentration and semen characteristics. Animal Reproduction Science. 84: 73–82.

Al-Shabbani, A.H.A., A. Dawood KH. and A. Jassem, (2013): Histopathological study of Trypanosomiasis in Camels of Al-Diwaniyah Province. AL-Qadisiya Journal of Vet. Med. Sci. 12:1.

Anosa, V.O. and J.J. Kaneko, (1984): Pathogenesis of *T. brucei* infection in deer mice (Peromyscus maniculatus) ultrastructural pathology of the spleen, liver, heart and kidney. Veterinary Pathology 24, 229–237.

Araque, W.H. (1985): *Trypanosoma venezuelense* en ratones: susceptibilidad a la infección y alteraciones de larespuesta inmune. Trabajo Especial de Grado de Maestría. Intituto Venezolano de Investigaciones Científicas. Caracas.

Ashour, A., T. Abou El-Naga, S. Barghash and M. Salama, (2013): *Trypanosoma evansi*: Detection of *Trypanosoma evansi* DNA in naturally and experimentally infected animals using TBR1 and TBR2 primers. Experimental Parasitology. 134: 109–114.

Bacchi, C. J. (2009): Chemotherapy of human African trypanosomiasis. Interdiscip. Perspect. Infect. Dis. 1–5.

Bal, M.S., L.D. Singla, H. Kumar, A. Vasudev, K. Gupta and P.D. Juyal, (2012): Pathological studies on experimental *Trypanosoma evansi* infection in Swiss albino mice. J. Parasitic Dis., 36: 260-264.

Baral, TN, P. Baetselier, F. Brombacher and S. Magez, (2007): Control of *Trypanosoma evansi* infection is IgM mediated and does not require a type I inflammatory response. J Infect Dis.; 195:1513–1520.

Biswas, D.; A. Choudhury and K.K. Misra, (2001): Histopathology of *Trypanosoma Trypanozoon evansi* infection in bandicoot rat. I. Visceral organs. Exp Parasitol. 99(3):148-59.1.

Brener, Z., (1962): Therapeutic activity and criterion of cure on mice experimentally infected with *Trypanosoma cruzi*. Rev. Inst. Med. Trop. Sao Paulo 4:389–396.

Carleton, M.A.; Durry, R.; Willington, E. and Cammeron, H. (1967): Carleton's histological techniques. 4th ed. Exford Univ. Press., New York.

Carmona, T.M.P., Garrizzo J., Roschman-González A., Tejero F., Escalante A.; Aso P.M. (2006): Susceptibility of different mouse strains to experimental infection with a Venezuelan isolate of *Trypanosoma evansi.* J. Protozool. Res. 16:1-8.

Chandra, D., B.N. Tripathi, R.V. Srivastava and R.K. Singh, (1999): Pathology of experimental *Trypanosoma evansi* infection in rabbits. Indian Journal of Veterinary Pathology 23:44-46.

Claes F., M. Radwanska, T. Urakawa, P.A. Majiwa, B. Goddeeris and P. Buscher, (2004): Variable surface glycoprotein RoTat 1.2 PCR as a specific diagnostic tool for the detection of *Trypanosoma evansi* infections. Kinetoplastid Biol. Dis. 3:3.

Dargantes A.P., S.A. Reid and D.B. Copeman, (2005a) Experimental *Trypanosoma evansi* infection in the goat. I. Clinical signs and clinical pathology. Journal of Comparative Pathology 133, 261-266.

Dargantes A.P., R.S. Campbell, D.B. Copeman and S.A. Reid, (2005b): Experimental *Trypanosoma evansi* infection in the goat. II. Pathology. Journal of Comparative Pathology 133, 267-276.

Dargantes A.P., R.T. Mercado, R.J. Dobson and S.A. Reid, (2009): Estimating the impact of *Trypanosoma evansi* infection (surra) on buffalo population dynamics in southern Philippines using data from cross sectional surveys. Int J Parasitol 39:1109–1114.

Dávila, A.M., H.M. Herrera, T. Schlebinger, S.S. Souza and Y.M. Traub-Cseko, Y.M., (2003): Using PCR for unraveling the cryptic epizootiology of livestock trypanosomosis in the Pantanal. Brazil. Vet. Parasitol. 117:1–13.

Desquesnes, M. and A.M.R. Davila, (2002): Applications of PCR-based tools for detection and identification of animal trypanosomes: a review and perspectives. Vet. Parasitol. 109, 213–231.

Desquesnes, M., P. Holzmuller, D. Lai, A. Dargantes, Z. Lun and S. Jittaplapong, (2013): *Trypanosoma evansi* and Surra: A Review and Perspectives on Origin, History, Distribution, Taxonomy, Morphology, Hosts, and Pathogenic Effects. BioMed Research International, Article ID 194176, 22 pages.

Faccio L., A.S. Da Silva, A.A. Tonin, L. Oberherr, L.T. Gressler, C.B. Oliveira, D.T. et al. (2014): Relationship between testicular lesion and hormone levels in male rats infected with Trypanosoma evansi. An Acad Bras Cienc: 86 (3).

Faccio, L.; A.S. Da Silva, A.A. Tonin, R.T. Franca, L.T. Gressler, M.M. Copetti, C.B. et al. (2013): Serum levels of LH, FSH, estradiol and progesterone in female rats experimentally infected by *Trypanosoma evansi*. Exp. Parasitol. 135, 110–115.

Gardiner, P.R. and M.M. Mahmoud, (1990): Salivarian trypanosomes causing disease in livestock outside sub-

saharan Africa. In: Baker J.R. Parasitic Protozoa, vol. 3. Academic Press, New York.

Hemeida, N.A., S.T. Ismail, and A.B. El-Wishy, (1985): Studies on testicular degeneration in the one-humped camel. In: Proceedings of the First Inter Cong. Appl. Sci., vol. 3, Zagazig, Egypt, pp. 450–458.

Holland, W.G., F. Claes, L.N. My, N.G. Thanh, P.T. Tam, D. Verloo, P. et al. (2001a): A comparative evaluation of parasitological tests and a PCR for *Trypanosoma evansi* diagnosis in experimentally infected water buffaloes. Vet. Parasitol. 97 (1), 23–33.

Ikede B.O., I. Fatimah, W.Sharifuddin and T.A. Bongso, (1983): Clinical and pathological features of natural *Trypanosoma evansi* infection in ponies in West Malaysia. Tropical Veterinarian,1, 151–153.

Konnai, S., H. Mekata, C.N. Mingala, N.S. Abes, C.A. Gutierrez, J.R. Herrera, A.P. et al. (2009): Development and application of a quantitative real-time PCR for the diagnosis of Surra in water buffaloes. Infect. Genet. Evol. 9:449–452.

Luna, L.G. (1986): Manual of histological staining methods of the armed forces institute of pathology. 3rd ed., Mc GRAW – HILL BOOK Company, New York.

Mekata H., S. Konnai, C. N. Mingala, N. S. Abes, C. A. Gutierrez, A. P. Dargantes, et al. (2012): Kinetics of regulatory dendritic cells in inflammatory responses during Trypanosoma evansi infection. Parasite Immunology. 34, 318–329.

Mekata H., S. Konnai, C.N. Mingala, N.S. Abes, C.A. Gutierrez, A.P. Dargantes, et al. (2013): Isolation, cloning, and pathologic analysis of Trypanosoma evansi field isolates. Parasitol Res 112:1513–1521.

Nantulya, V.M. (1990): Trypanosomiasis in domestic animals: the problems of diagnosis. Rev. Sci. Tech. Off. Int. Epizoot., 9: 357–367.

OIE (2012): *Trypanosoma evansi* infection (SURRA). Terrestrial Manual, Chapter 2.1.17.

Pradhan S., S.S. Roy and S.K. Mukhopadhyaya, (2013): Effect of experimental *Trypanosoma evansi* on fertility in Black Bengal Buck*. Indian Journal of Animal Sciences* 83 (7): 688–692.

Ramírez-Iglesias, J.R., M.C. Eleizalde, M. Gómez-Piñeres, E. and M. Mendoza (2011): *Trypanosoma evansi*: A comparative study of four diagnostic techniques for trypanosomosis using rabbit as an experimental model. Experimental Parasitology 128: 91–96.

Ramírez-Iglesias J.R., M.C. Eleizalde, E. Gómez-Piñeres and M. Mendoza (2012): *Trypanosoma evansi*: A clinical, parasitological and immunological evaluation of trypanosomosis using a chronic rabbit model Open Veterinary Journal, 2: 78-82.

Rjeibi M.R., Ben Hamida T., Dalgatova Z., Mahjoub T., Rejeb A., Dridi W., and Gharbi M. (2015): First report of surra (*Trypanosoma evansi* infection) in a Tunisian dog: Parasite, 22: 3.

Sackey A. K. (1998): Comparative study of trypanosomosis experimentally induced in Savanna Brown bucks by *Trypanosoma bruci, T. congolense and T. vivax*. Ph.D. thesis, Ahmado Bello, Univ., Zaria.

Saleh, M.A, M.A. Bassam and S.A. Sanousi, (2009): Oxidative stress in blood of camels (Camelus dromedaries) naturally infected with *Trypanosoma evansi*. Vet Parasitol; 162: 192–9.

Sambrook, J. and D.W. Russell (2001): Molecular Cloning: A laboratory Manual. Cold Spring Harbor Laboratory Press, Cold Spring Harbor, NY.

Sarataphan, N., K. Unjit, M. Vongpakorn and P. Indrakamhaeng (2007): Real-Time PCR for detection of *Trypanosoma evansi* in blood samples using SYBR Green I fluorescent dye. In: Proceeding Developing Methodologies for the Use of Polymerase Chain Reaction in the Diagnosis and Monitoring of Trypanosomosis, IAEA-TECDOC-1559, pp. 93–102.

Sengupta, P.P., M. Balumahendirana, W. Suryanaryanab, A.G. Raghaven-dra, B.R. Shomea, M.R. Gajendragada and K. Prabhudas (2010): PCR-based diagnosis of surra-targeting VSG gene: experimental studies in small laboratory rodents and buffalo. Vet. Parasitol. 171, 22–31.

Shams El-Din A. Salwa, (2012): *Effect of Human Immunogloblins on Experimental Murine Trypano-somiasis Caused by Trypanosoma evansi.* PUJ; 5(1): 11-18.

Sharma P., P.D. Juyal , L.D. Singla , D. Chachra and H. Pawar (2012): Comparative evaluation of real time PCR assay with conventional parasitological techniques for diagnosis of *Trypanosoma evansi* in cattle and buffaloes. Vet Parasitol. ; 190 (3-4): 375-382.

Shumei, Z. Yongzhi, Z. Yunfei, W. and Renjian, Z., (1996): Comparative study on different methods of preserving *Trypanosoma evansi* by liquid nitrogen cryofreezing. Chinese Journal of Veterinary Parasitology. 1996-04.

Sukhumsirichart, W., S. Khuchareonaworn, N. Sarataphan, N. Viseshakul and K. Chansiri, (2000): Application of PCR-based assay for diagnosis of *Trypanosoma evansi* in different animals and vectors. J. Trop. Med. Parasitol. 23:1-6.

Suryanarayana, C., S.L. Gupta, R.P. Singh and J.R. Sadana (1986): Pathological changes in donkeys (*Equus asinus*) experimentally infected with *T. evansi. Indian Veterinary Medical Journal* 6, 57–59.

Tejero, F., Roschman-González, A., Perrone-Carmona, T.M. and Aso, P.M. (2008): *Trypanosoma evansi:* A quantitative approach to the understanding of the morphometry-hematology relationship throughout experimental murine infections. J. Protozool. Res. 18, 34-47.